

Solving Kepler’s equation with CORDIC double iterations[★]

M. Zechmeister^{★★}

Institut für Astrophysik, Georg-August-Universität, Friedrich-Hund-Platz 1, 37077 Göttingen, Germany

Accepted 2020 August 6. Received 2020 August 5; in original form 2020 May 11.

ABSTRACT

In a previous work, we developed the idea to solve Kepler’s equation with a CORDIC-like algorithm, which does not require any division, but still multiplications in each iteration. Here we overcome this major shortcoming and solve Kepler’s equation using only bitshifts, additions, and one initial multiplication. We prescale the initial vector with the eccentricity and the scale correction factor. The rotation direction is decided without correction for the changing scale. We find that double CORDIC iterations are self-correcting and compensate possible wrong rotations in subsequent iterations. The algorithm needs 75% more iterations and delivers the eccentric anomaly and its sine and cosine terms times the eccentricity. The algorithm can be adopted for the hyperbolic case, too. The new shift-and-add algorithm brings Kepler’s equation close to hardware and allows to solve it with cheap and simple hardware components.

Key words: celestial mechanics – methods: numerical

1 INTRODUCTION

Kepler’s equation (KE) is fundamental in many fields of astrophysics. It relates mean anomaly M and eccentric anomaly E via the equation

$$E - e \sin E = M(E) \quad (1)$$

where $M(t) = \tau \frac{t}{P}$ with time t and orbital period P .

In practice we often need to solve the inverse the problem $E(M)$. For instance, in orbit fitting, observing times t are given and then the location or velocity of an object must be predicted, which then requires to compute E .

Many methods have been proposed to solve KE, such as Newton iterations, Halley’s method, table interpolation, or inverse series (Colwell 1993). In Zechmeister (2018, hereafter Ze18), we proposed to use a CORDIC-like algorithm. CORDIC (Coordinate Rotation Digital Computer) was invented by Volder (1959) and can compute many elementary functions (e.g. cosine, sine, multiplication)¹ and needs only additions and bitshifts. We will briefly review the CORDIC concept in Sect. 2.

In Ze18, the rotation directions are set accurately. However, already this step requires a multiplication in each iteration. To overcome this shortcoming, we study here the idea to simply ignore the scale change in the direction decision, still hoping for a correct convergence (Sect. 3). We will demonstrate that this approach is indeed purposeful given some appropriate adjustments. Finally, we

discuss an implementation (Sect. 5) and evaluate the performance of the algorithm (Sect. 6).

2 CORDIC ALGORITHM FOR ELEMENTARY FUNCTIONS

A complex number can be expressed in Cartesian coordinates

$$z = x + iy \quad (2)$$

as well as in polar coordinates

$$z = r \exp i\varphi \quad (3)$$

where $x = r \cos \varphi$ and $y = r \sin \varphi$.

When we represent this number z by a sequence of rotations with angles θ_n , these are simple additions in the exponent in the polar representation or complex multiplications in the Cartesian representation

$$r e^{i \sum \theta_n} = z = r \prod_n (\cos \theta_n + i \sin \theta_n). \quad (4)$$

Additions are very easy to perform for computers, while multiplications are usually more expensive, in particular with simple hardware as years ago. Therefore, Volder (1959) sought to simplify the product in Eq. (4). He factored the term $\cos \theta_n$

$$z = r \prod_n \cos \theta_n \prod_n (1 + i \tan \theta_n) \quad (5)$$

and allowed only angles of the form

$$\theta_n = \sigma_n \alpha_n \quad (6)$$

[★] Code available at <https://github.com/mzechmeister/ke/>.

^{★★} E-mail: zechmeister@astro.physik.uni-goettingen.de

¹ We provide an online demo at <https://raw.github.com/mzechmeister/ke/master/cordic/js/cordic.html>.

with

$$\tan \alpha_n = \frac{1}{2^{n-1}} \quad \text{and} \quad \sigma_n \in \{-1, 1\} \quad (7)$$

for $n \geq 1$. So the first angle is $\alpha_1 = 45^\circ$ and the next rotation angles α_n are almost halved in each iteration and the rotation can be clock- or counter-clockwise (positive or negative). Now, Eq. (5) can be written as

$$z = rK_N \prod_n \left(1 + i \frac{\sigma_n}{2^n}\right) \quad (8)$$

where the term

$$K_N = \prod_n \cos \alpha_n = \prod_n \frac{1}{\sqrt{1 + \tan^2 \alpha_n}} = \prod_n \frac{1}{\sqrt{1 + 4^{-n}}} \quad (9)$$

is called scale correction. The factor K_N can be pre-computed, because the cos-function is symmetric and therefore independent of σ_n and the absolute values of the rotation angles $|\theta_n| = \alpha_n$ are pre-defined ($K_c \equiv K_\infty \approx 0.607253$)².

Due to the angle choice in Eq. (7), the remaining product term can be computed efficiently. This is easier to explain when explicitly writing an adjacent rotation for the real and imaginary part of z as

$$x_{n+1} = x_n - m \frac{\sigma_{n+1} y_n}{2^{k_{n+1}}} \quad (10)$$

$$y_{n+1} = y_n + \frac{\sigma_{n+1} x_n}{2^{k_{n+1}}}, \quad (11)$$

where the coordinate parameter m is 1 for the circular case (-1 for the hyperbolic and 0 for the linear case).

The multiplication with σ_n is just a negation in case $\sigma_n = -1$. The multiplication by an integer power of two (2^{-n}) is also very easy for a computer. It is a simple bit shift in binary system; very similar in a decimal system a division by ten is just a left shift of the decimal point. Therefore, all multiplications are eliminated. Only the one multiplication rK_N in Eq. (8) remains; and in case $r = 1$ even this multiplication can be saved (Walther 1971); the start vector is initialised with $(x_0, y_0) = (K_N, 0)$.

With these basic equations, the CORDIC algorithm can compute the sine and cosine function. Given an input angle φ , we can approach it in each iteration with the condition

$$\sigma_{n+1} = \begin{cases} +1 & \sum \theta_n < \varphi \\ -1 & \text{else.} \end{cases} \quad (12)$$

The Cartesian representation is propagated simultaneously with the same rotation directions σ_n via Eqn. 10 and 11. So when $\sum \theta_n \rightarrow \varphi$, then $x_n \rightarrow \cos \varphi$ and $y_n \rightarrow \sin \varphi$. Figure A1 illustrates this process.

The convergence range can be derived when performing only positive rotations resulting in $\sum_{n=1}^N |\theta_n| = \sum_n \arctan 2^{-(n-1)} \rightarrow 1.7433 = 99.88^\circ$ for $N \rightarrow \infty$. An initial rotation with 90° , which needs no scale correction, can extend the range to 189.88° .

It is also possible to calculate $\text{atan}(x, y)$. So given x and y , the angle φ of this vector is wanted. In this mode, called vectoring, the component y_n is driven towards zero.

² The q -Pochhammer symbol is defined as $(a; q)_n = \prod_{k=0}^{n-1} (1 - aq^k)$. Thus the product series $K_c^2 = \prod_{k=0}^{\infty} (1 + 4^{-k})$ is the special case $(-1; \frac{1}{4})_{\infty} \approx 2.71182$. Likewise, in hyperbolic mode there occurs $\prod_{k=1}^{\infty} (1 - 4^{-k}) = (\frac{1}{4}; \frac{1}{4})_{\infty} \approx 0.68854$, which is also a special case of the Euler product.

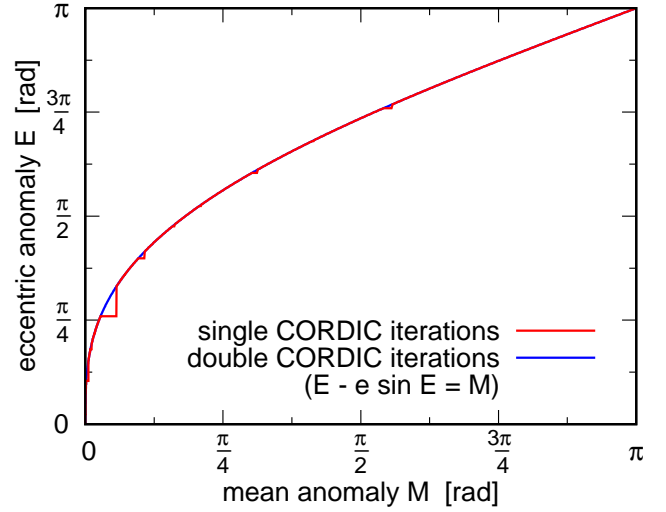


Figure 1. CORDIC on KE (for $e=1$) with single iterations (red, shift sequence $k_n = 0, 1, 2, 3, 4, \dots$) and with double iterations (blue, $k_n = 1, 1, 2, 2, 3, 3, \dots$).

Walther (1971) generalised the CORDIC algorithm with a linear and hyperbolic mode allowing to compute multiplication, division and the functions \exp , \ln , atanh , and square root. Table A1 gives an overview of the different modes and Table A2 lists the required input and the corresponding output to obtain various elementary functions. This diversity demonstrates the capability of this simple algorithm.

However, it must be noted that the hyperbolic mode needs specific iterations to be done twice for³

$$k_n \in 4, 13, 40, 121, \dots, K, 3K + 1 = \frac{3^{m+2} - 1}{2}. \quad (13)$$

This compensates the accumulating problem that subsequent rotation angles are a little smaller than half, $2\alpha_{n+1} < \alpha_n$ (while the circular modes has here some redundancy $2\alpha_{n+1} > \alpha_n$, and the linear mode is exact $2\alpha_{n+1} = \alpha_n$). With this sequence the convergence is overall. From now on, we use the variable name n for iteration number and k_n for the shift sequence.

3 CORDIC DOUBLE ITERATIONS FOR KEPLER'S EQUATION

To apply CORDIC to Kepler's equation, we proposed in Ze18 the modified condition for the rotation direction⁴

$$\sigma_{n+1} = \begin{cases} +1 & E_n - e \sin E_n < M \\ -1 & \text{else.} \end{cases} \quad (14)$$

For readability and with respect to Eq. (1), we renamed $\sum \theta_n$ with E_n and φ with M compared to Sect. 2.

The decision in Eq. (14) is exact within the working precision. However, the term $\sin E_n$ is not accessible in true CORDIC, because of the scale change. And a simultaneous compensation would require a multiplication in every iteration. When the start vector

³ The sequence is related to <http://oeis.org/A003462>.

⁴ For reasons of uniformity with code implementation, we list the positive case first compared to Ze18.

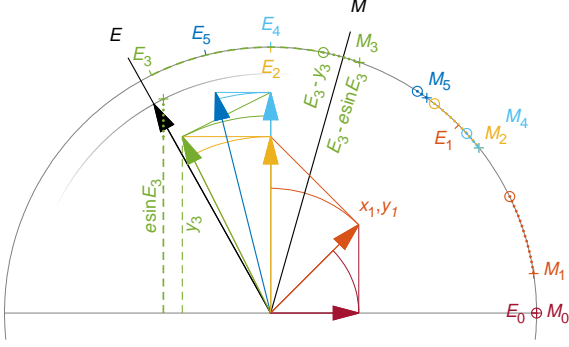


Figure 2. Evolution of the vector x_n, y_n (colour-coded arrows), when dropping the scaling term $\cos \alpha_n$ and using double rotation. The example is for $e=0.9$ and $M=2.08-0.9 \sin 2.08 \approx 1.294$ (thus $E=2.08$). With appropriate prescaling by K_N , the vector approaches length e (grey arc) after $n=N$ (black arrow) and converges towards the E . The discrepancy between exact intermediate mean anomaly $M_n = E_n - e \sin E_n$ (crosses) and approximated mean anomaly $E_n - y_n$ (open circles) is colour-coded with dotted arcs on the grey unit circle. Iteration $n=1$ and $n=2$ (or three and four) have the same angle α_n .

$E_0=0$ is pre-scaled with K_N , i.e.

$$x_0 = K_N e \cos E_0 = K_N e \quad (15)$$

$$y_0 = K_N e \sin E_0 = 0, \quad (16)$$

then the term y_n converges towards $e \sin E_n$ for $n \rightarrow N$. But at iteration n , the relation is

$$y_n = \frac{K_n}{K_N} e \sin E_n.$$

Therefore, y_n and $e \sin E_n$ deviate by the factor $\frac{K_n}{K_N} = \prod_{n=1}^N (1 + 4^{-k_n})^{-1/2}$ (in double precision it is negligible for $k_n \geq 27$).

In this work, we simply propose

$$\sigma_{n+1} = \begin{cases} +1 & E_n - y_n < M \\ -1 & \text{else.} \end{cases} \quad (17)$$

This ignores totally the changing scale. Still, we might hope for a convergence. Figure 1 shows what happens for the extreme case of $e=1$. Many regions seem to converge, but obviously others do not converge. The approximation leads sometimes to rotations into wrong directions and the subsequent rotations seem not to overcome this.

There are other functions that can have similar issues, for instance the arcsine (Muller 2006). Baykov (1972) solved the problem with double iterations, meaning each iteration is executed twice. In Sect. A1, we discuss the arcsine function.

We continue investigating the approach of Baykov (1972), because it does not require any modifications of the CORDIC algorithm besides the sequence for k_n . We also remind that the hyperbolic mode needs specific iterations to be repeated, too. So double iteration is an established workaround. Indeed it turns out, that the double iterations also work for Kepler's equation (Fig. 1).

We can explain the success as follows. As already mentioned, y_n is a good approximation of $e \sin E_n$. A rotation into a wrong direction can occur, when the intermediate angle is already close to the target value (see $n=3$ in Fig. 2). Then the true $M_n = E_n - e \sin E_n$ and the approximation $E_n - y_n$ may lay on different sides with respect to the target M (see Fig. 2, a positive rotation $\sigma_4 = +1$ would be needed according to M_3 , but $E_3 - y_3$ suggests $\sigma_4 = -1$). A wrong rotation moves away by at least α_n and needs to be compensated by

the subsequent rotations. In case of single rotations, all subsequent rotations $\sum_{n+1} \alpha_n \approx 2\alpha_{n+1}$ can recover α_n . But the small redundancy in single rotations (in $m=1$) is generally insufficient to compensate yet the initiating departure. Double rotations, however, introduce redundancy, which is the key to overcome the convergence problem, but also the price to be paid for the approximation.

4 HYPERBOLIC MODE

Analogous to Ze18, we study whether our double iteration algorithm is also applicable to the hyperbolic Kepler's equation (HKE)

$$M = e \sinh H - H, \quad (18)$$

where $e \geq 1$. Replacing the trigonometric terms by the hyperbolic analogues, Eqn. 7 and 17 become

$$\tanh \alpha_n = \frac{1}{2^{k_n}} \quad (19)$$

$$\sigma_{n+1} = \begin{cases} +1 & y_n - H_n < M \\ -1 & \text{else.} \end{cases} \quad (20)$$

With $m=-1$ in Eq. (10), hyperbolic rotations are performed. The hyperbolic iterations return $x_N = e \cosh H_N$ and $y_N = e \sinh H_N$. The double iterations cover a range of $|H| < 2.111$ (in Ze18: $|H| < 4 \ln 2 = 2.772$). The scale correction is $K_{h,dbl} \approx K_{h,\infty}^2 (1 - 4^{-4}) \approx 1.45235$. As suggested in Ze18, large mean anomalies can be handled with appropriate start values

$$H_0 = k_0 \ln 2 \quad (21)$$

$$x_0 = K e \cosh H_0 = \frac{eK}{2} [\exp H_0 + \exp(-H_0)] \quad (22)$$

$$= eK [2^{k_0-1} + 2^{-k_0-1}] \quad (23)$$

$$y_0 = K e \sinh H_0 = \frac{eK}{2} [\exp H_0 - \exp(-H_0)] \quad (24)$$

$$= eK [2^{k_0-1} - 2^{-k_0-1}]. \quad (25)$$

where the integer k_0 is taken from

$$k_0 = \text{sign } M \cdot \max \left[0, \text{floor} \left(1 + \log_2 \left| \frac{M}{e} \right| \right) \right]. \quad (26)$$

We remark that, the start triple requires only additions and bitshifts and the one multiplication in eK . For $k_0=0$, the start triple is similar to the elliptic case ($H_0=0$, $x_0=1$, and $y_0=0$). For $k_0 \neq 0$, the triple yields a range extension. (A range reduction as in the circular case, where E_0 and y_0 becomes zero, is not possible.)

5 IMPLEMENTATION AND VARIANTS

We have indicated in the previous section that our algorithm can solve Kepler's equation. Here we comment about some details of the implementation. In particular, we briefly explain the properties of fixed-point and floating-point representation and the consequences for the algorithm. The discussion brings us close to the basics of computer architecture.

5.1 Fix-point implementation

CORDIC was originally invented for systems with fixed-point numbers. In fixed-point, a float number is mapped linearly into a chosen integer range. A 64 bit system can represent about $2^{64} \approx$

Table 1. Examples for bit operations (arithmetic shift, xor, and) in two's complement with 8 bits.

input	operation	output	decimal expression
0000 0001	<<2	0000 0100	$1 \times 2^2 = 4$
1111 1111		1111 1100	$-1 \times 2^2 = -4$
0000 1011	>>2	0000 0010	$11 / 4 = 2$
1111 0101		1111 1101	$-11 / 4 = -3$
0111 1111	$\wedge(-1)$	1000 0000	$127 \wedge (-1) = -128$
0111 1111	$\wedge 0$	0111 1111	$127 \wedge 0 = 127$
1111 0101	$\&(-1)$	1111 0101	$-11 \& (-1) = -11$

$1.8 \cdot 10^{19}$ numbers. The location of the virtual “binary point” depends on the convention for the mapping function.

Most systems operate with two's-complement arithmetic. That means, for signed integers the leading bit is preserved to distinguish positive and negative numbers. The bit is set for negative numbers. In particular, -1 is represented by setting all bits (Table 1, second row). There is one more negative number than positive numbers (e.g. -128 vs. 127 in 8 bit systems).

A multiplication or a division by a power of two (2^n) is done quickly by a bitshift to the left or right, respectively. (Similarly, in decimal system a division by 10^n is just a left shift of the decimal point). This is illustrated in Table 1. A right shift of the digits performs a division with a round-down (floor). Therefore, it should not surprise that, for instance, $-11/4 = -3$.

The multiplication with ± 1 can be implemented in software with a conditional addition/subtraction via an if-statement. A branchless alternative is implemented in Code B.1 and Code B.2.

In both elliptic and hyperbolic case, we can set the binary point between the 62th and 61th bit. The most significant bit (number 64th) is used as sign bit. Then next two bits (63 and 62) can represent $2^1 = 2$ and $2^0 = 1$. This together with the fractional bits covers a range of $\pm(4 - 2^{-61})$ and thus includes the convergences range of $\pm \frac{\pi}{2}$ and ± 2.111 , respectively.

5.2 Floating-point implementation

Nowadays, float numbers on desktop computers are usually represented in floating-point format as specified in IEEE 754 (IEEE 2008). Here the first bit is the sign bit, followed by the exponent bits and finally the mantissa.

One possibility to apply CORDIC is to simply convert the float numbers to fixed-point representation and to continue with Sect. 5.1. This concept is realised in Code B.1 and in Code B.2.

If the algorithm should be still carried out with floating-point format, one can consider the following circumstances. A multiplication with -1 is just a flip of the sign bit. A division by 2^k is just a subtraction of k from the exponent. However, one has to catch the possibility of an exponent underflow. Also, the addition of two floating point numbers requires an internal normalisation of the exponent. Hence addition is not much faster than multiplication and both usually slower than fix-point addition.

5.3 Shift and angle sequence

When we chose as shift sequence $k_n = 0, 0, 1, 1, 2, 2, \dots$ for the circular mode, then double iterations cover a range of $|E| < \sum_{n=1}^N \alpha_n \approx 199.88^\circ$, that means about twice as wide as in single rotations. The scale factor becomes $K_{\text{dbl}} \approx K_\infty^2 = 0.368\,76$.

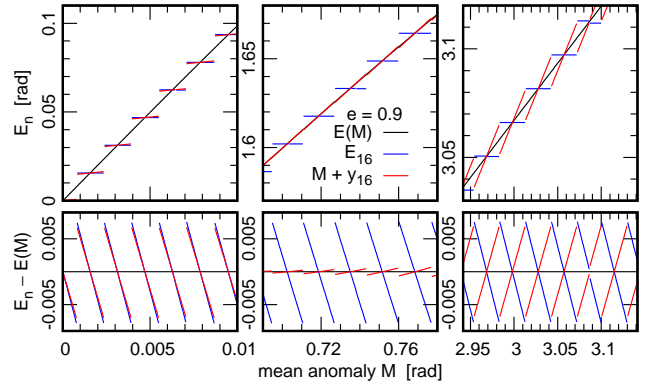


Figure 3. Top: CORDIC output after 16 double iterations ($k_{16} = 8$, 29 fractional bits) for eccentricity $e = 1$ and three mean anomaly regions. Compared to the exact solution E (black), E_{16} is a step function (blue), while $M + y_{16}$ (red) has slopes. Bottom: The absolute residuals are smaller than $2^{-7} = 0.0078125$.

Alternatively, one can also start with one scale-free pre-rotation with $\alpha_1 = 90^\circ = \frac{\pi}{4}$ in exchange for two rotations with $\alpha_1 = \alpha_2 = 45^\circ$ ($k_1 = k_2 = 0$)

$$\sigma_1 = \begin{cases} +1 & E_0 - e \sin E_0 < M \\ -1 & \text{else} \end{cases} = \begin{cases} +1 & E_0 < M \\ -1 & \text{else} \end{cases} \quad (27)$$

$$E_1 = E_0 + \sigma_1 \frac{\tau}{4} \quad (28)$$

$$x_1 = x_0 \cos \frac{\tau}{4} - \sigma_1 y_0 \sin \frac{\tau}{4} = -\sigma_1 y_0 = 0 \quad (29)$$

$$y_1 = y_0 \cos \frac{\tau}{4} + \sigma_1 x_0 \sin \frac{\tau}{4} = \sigma_1 x_0 = \sigma_1 e K \quad (30)$$

Combined with the sequence $k_n = 1, 1, 2, 2, 3, 3, \dots$, the convergence range remains the same and the scale factor becomes $K_{\text{dbl}} \approx (\frac{1}{\cos 45^\circ} K_\infty)^2 = 2K_\infty^2 = 0.737\,51$. Obviously, the relative speed profit decreases with number of total iterations.

5.4 Accumulation

The condition $E_n - y_n < M$ in Eq. (17) is internally likely evaluated as $M - E_n + y_n > 0$ and therefore requires two subtractions (and one comparison). It can be advantageous to reformulate this as $t_n + y_n > 0$ with $t_n = M - E_n$ and $t_0 = M$. This saves one subtraction (and one variable i.e. memory access) in each iteration and is possible, because M is a fixed input and E_n is needed only in the comparison during the iterations. This accumulation is a common practice in CORDIC algorithms, where for $e = 0$ (so $y_n = 0$) the condition $t_n > 0$ remains. At the end the eccentric anomaly can be recovered with $E_N = M + y_N$.

Figure 3 shows that the output $M + y_N$ differs a bit from E_N , but both are within the nominal limits. Positive and negative residuals appear balanced with no visible bias for both cases; a property related to the two-sided design of the proposed CORDIC algorithm (see also Fig. 3 of Ze18). Contrary, one-sided algorithms will be biased. Such a variant was outlined in Ze18 (Eq. (13)).

6 ACCURACY AND PERFORMANCE STUDY

6.1 Accuracy of the fix-point algorithm

We forward calculated with Eq. (1) 1 000 ($M(E)$, E) pairs, with M sampled log-uniformly over $[10^{-26}, \frac{\pi}{2}]$. Here E might be seen as

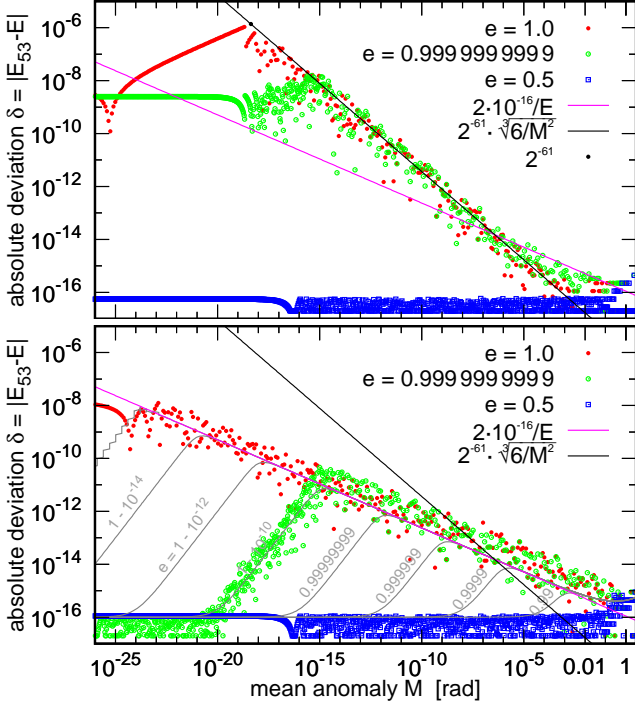


Figure 4. Accuracy for the fix-point (top) and floating-point algorithm (bottom). For visibility, zero deviations ($\delta = 0$) were lifted to $\delta = 2 \cdot 10^{-17}$.

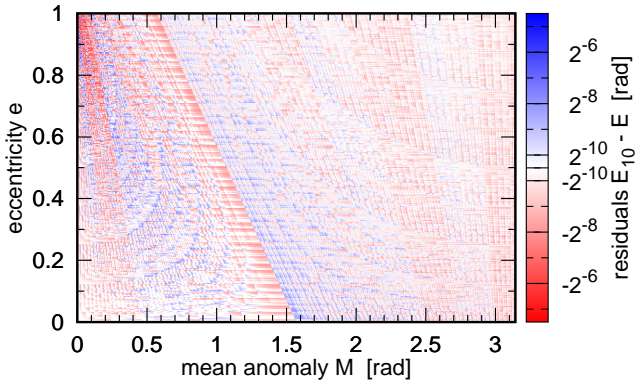


Figure 5. Residual map for a fix-point algorithm with 10 fractional bits and iterated to the last bit ($k_N = k_{17} = 10$). The colour-coding is log-symmetric.

the true value. Then we injected M into our algorithms to solve the inverse problem $E(M)$. The top panel of Fig. 4 shows the dependency of the accuracy as function of M and e for Code B.1. The accuracy becomes critical in the so called corner of KE at $M=0$ for $e=1$. Here the function behaves like a cubic root $E \approx \sqrt[3]{6M}$ and the derivative becomes infinite. When using 61 bits for the binary fraction (Sect. 5.1), the step size is $2^{-61} = 4.3 \cdot 10^{-19}$ rad. This is the resolution for M . The value of the eccentric anomaly is $\Delta E = E(M = \Delta M) = \sqrt[3]{6 \cdot 4.3 \cdot 10^{-19}} = 1.4 \cdot 10^{-6}$. This point marks about the largest error and is indicated in the figure.

The general error relation is $dE = \frac{1}{1-e \cos E} dM$, which follows from Eq. (1). For $e=1$, it becomes $dE \approx \frac{1}{3} \sqrt{\frac{6}{M^2}} dM$ and since ΔM is constant, the errors declines as $\propto M^{-2/3}$. The residuals matches those theoretical limits and thus validates our implementation.

We remind, that Fig. 4 is an extreme magnification of the cor-

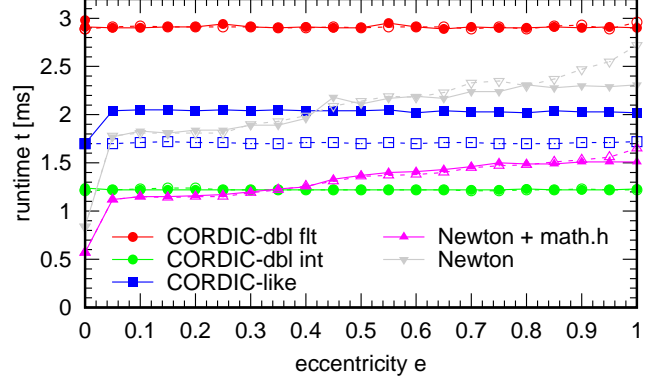


Figure 6. Execution time as function of eccentricity for various algorithms. For solid curves, M was distributed uniformly, for dashed curves E .

ner. The errors decrease quite quickly with eccentricity. The increase of error for $M \gtrsim 0.1$ should be related to the simplified conversion between floating-point and fix-point, which was used for the preparation of the look-up table and the input data. The mantissa of 64 bit floating-point numbers holds only 53 bits.

Finally, we remark the need for some spare bits. This is investigated here with a short bit system. We divided the range from 0 to 4 rad into $2^{12} = 4096$ mean anomalies having thus 10 fractional bits (2^{-10}). Then we limited our fix-point algorithm also to 10 fractional bits (cf. L 12 in Code B.1) and iterated until the last bit, i.e. $k_N = 10$ ($N = 17$). Still, the residuals in Fig. 5 are overall limited to 2^{-6} (with a slight bias towards more negative deviations) for this short bit algorithm. So sometimes the last four iterations yield no improvement. Therefore, some trailing bits ($\sim \log_2 k_N$) are advisable to buffer accumulating truncation errors.

6.2 Accuracy of the floating-point algorithm

Overall, the error behaviour of the floating-point algorithm with double iteration (Fig. 4) is very similar to the CORDIC-like algorithm from Ze18 (Fig. 6), who already explained the functional forms arising for the different eccentricities. Compared to the fix-point algorithm, the floating-point algorithms have a better accuracy in the corner, where they profit from the higher precision to represent small numbers. On the other hand, the fix-point version has better accuracy at about $M \gtrsim 10^{-5}$.

The algorithm used for Fig. 4 employed the shift sequence starting with $k_n = 0, 0, 1, 1, 2, 2, \dots$ and without accumulation. For small mean anomalies, the rotation will go back and forth to zero in the first iterations, thus keeping properties of the one-sided algorithms in Ze18. However, the two optimisations suggested in Sect. 5.3 and Sect. 5.4 will worsen the accuracy to a level comparable to the fix-point algorithm, because for floating-point the order of additions does matter (while in fix-point format this does not affect the precision). Both cases lead to the additions of small numbers to big numbers, and thus floating-point numbers cannot utilise the better representation of small numbers.

6.3 Performance

We have shown that Kepler's equation can indeed be solved with the shift-and-add algorithm CORDIC using minor modifications. Thus, the pressing question is: how fast is the algorithm?

We implemented the algorithms (as well as the comparison

solvers) in plain C and measured with the Python’s `timeit` feature the execution times to solve Eq. (1) 10 000 times and for 21 eccentricities between 0 and 0.999 999. The maximum shift index in the CORDIC versions was $k_N = 28$ corresponding to a precision of $2^{-28} = 3.7 \cdot 10^{-9}$. The mean anomalies M were distributed uniformly between $0 \dots 180^\circ$ (case $\mathcal{U}(M)$). In a second test, mean anomalies were generated, whose eccentric anomalies E were distributed uniformly (case $\mathcal{U}(E)$). This gives some more weight to small mean anomalies and shall probe whether there is a dependency on M , since some solvers are slower in the corner.

Figure 6 shows the results. The CORDIC double rotation algorithms performed $N_{\text{dbl}} = 56$ iterations⁵. The runtime is independent of eccentricity and the mean anomaly. The fix-point version is about 2.2 times faster than the floating-point version. Thus there is a noticeable benefit. However, it is also “only” a factor of two, since the floating-point code needs two multiplications in each iterations. This shows that multiplications have been optimised over the last years in current computer processing unit (CPU), crowded out CORDIC algorithms from those architectures.

For comparison, we show the CORDIC-like version from Ze18, which is a floating-point algorithm. We used a one-sided variant, which is faster for small E . This may partly explain the performance increase for the case $\mathcal{U}(E)$. Moreover, this version used an if-branch, thus branch prediction may affect the results, too. In any case, since the CORDIC-like version needs only $N = 29$ iterations, it is faster than its double iteration companion. Yet, the new fix-point version is even 1.5 times faster.

Finally, we see that the speed of the fix-point version compares well with Newton’s method, which used the start guess $E_0 = M + 0.85e$. The cosine and sine functions were called from the standard `math.h` library. Since the source of their implementation can be hard to track down, a self-programmed sine and cosine functions were tested as well. The runtime increases with eccentricity. At $e = 1$, the $\mathcal{U}(E)$ case take a bit longer than the $\mathcal{U}(M)$ case, which indicates slower convergence in the corner (at $M \approx 0$).

The performed tests can only serve as an orientation. There are many aspects, which can alter the outcome. Furthermore, the algorithm in Ze18 yields as output also the terms $\cos E$ and $\sin E$, which will be needed for subsequent computation. Our CORDIC algorithm delivers $e \cos E$ and $e \sin E$. In case division by e appears disadvantageous in particular for small eccentricities, one can recompute the terms from E or alternatively propagate them in parallel with the algorithm.

7 FURTHER DISCUSSION

7.1 Unifying the Keplerian CORDIC modes

CORDIC has three coordinate systems: linear, circular, and hyperbolic. We have extended here the circular and hyperbolic mode to the elliptic and hyperbolic case of Kepler’s equations. Thus, the question is nearby, whether there is an analog extension for the linear mode. To address this, we summarise the main difference in the

input and the direction decision of the various modes

$$\text{rotating} \quad t_n > 0 \quad t_0 = \varphi \quad (31)$$

$$\text{vectoring} \quad -y_n > 0 \quad t_0 = 0 \quad (32)$$

$$\text{arcsine} \quad -\varphi + y_n > 0 \quad t_0 = 0 \quad (33)$$

$$\text{KE} \quad t_n + y_n > 0 \quad t_0 = M \quad (34)$$

$$\text{HKE} \quad -t_n - y_n > 0 \quad t_0 = -M, \quad (35)$$

which includes the arcsine mode for completeness. The Keplerian modes appear as mixture of rotating and vectoring, and we call it “keplerling”.

Rotation and vectoring handle the different coordinate systems via the parameter m , which appears in Eq. (10), but not in Eqn. 31–33. Now, to unify the Keplerian modes, we can suggest to introduce m in Eqn. 34 and 35 as

$$\text{GKE} \quad m(t_n + y_n) > 0 \quad t_0 = mM. \quad (36)$$

For the linear mode with $m = 0$, this unification appears pointless, as the outcome will not depend on M at all. Well, if we associate the linear Keplerian mode with the case of *radial trajectories*, it would indeed complete the picture. KE and HKE solve for a time dependent auxiliary angle, but in radial cases the angle is fixed and time independent.

Another possibility for unification are base angles $m\alpha_n$ (thus negative for HKE) along with the condition $t_n + my_n > 0$ and $t_0 = M$. Then for $m = 0$, all base angle would be zero.

7.2 Barker’s equation

We also considered that a linear mode extension might be associated with parabolic orbits. This special case is handled with Barker’s equation (Colwell 1993), which is given by

$$M = D + \frac{1}{3}D^3, \quad (37)$$

where D is an auxiliary variable, similar to the eccentric anomaly E and H , and related to true the anomaly by

$$\tan \frac{\nu}{2} = D. \quad (38)$$

Equation (37) is a cubic equation, whose explicit solution is often given as

$$D = B - \frac{1}{B} \quad (39)$$

with $B = \sqrt[3]{W + \sqrt{W^2 + 1}}$ (Meire 1985) and $W = \frac{3}{2}M$. Computing this in a CORDIC framework requires five operations: division, hypotenuse, as well as exp, div, and ln for the cubic root ($3M$ are simply three additions).

The equivalent solution with hyperbolic functions

$$D = 2 \sinh \frac{\operatorname{asinh} \frac{3M}{2}}{3} \quad (40)$$

seems to be less known (Sect. C). It requires at most five CORDIC operations: sinh, div, and, for the arcsine hyperbolicus (Eq. (A3)), mul, cathetus, and atanh. When using the double iteration variant for the arcsine hyperbolicus, then the total costs are about four CORDIC cycles. A further reduction could be done by optimising the division by three (Sect. A2).

Therefore, Barker’s equation can be solved with a few nested CORDIC operations, but we don’t see a possibility to tackle it more directly with CORDIC.

⁵ For simplicity, we just truncated the shift sequence of the $k_N = 61$ version, which performs double iterations until $k \leq 26$, thus $N_{\text{dbl}} = 2 \cdot 27 + (28 - 26) = 56$. But already for $k > 14$, scale corrections are smaller than $4^{-14} = 2^{-28}$. Thus $N_{\text{dbl}} = 2 \cdot 15 + (28 - 14) = 44$ would be sufficient, too, promising a 21 % shorter runtime.

8 SUMMARY

In this work, we presented to our knowledge for the first time a shift-and-add algorithm to solve KE. The features of the algorithm are

- usage of most basic computer operations (addition, bitshift, xor)
- small code size and short lookup table
- independent of math libraries
- adjustable precision
- runtime independent of mean anomaly M and e .

We require only two minor modifications to the normal CORDIC algorithm, which are the modified direction decisions (Eq. (17)) and repeating each iteration once (double iterations for $k \leq \frac{1}{2}k_N$). The modifications constitute a new CORDIC mode, which we call Keplerian mode or keplerling. It is mixture of rotating and vectoring and handles the eccentric and hyperbolic case of Kepler's equation.

From the perspective of CORDIC, solving Kepler's equation appears twice as expensive as the computation of a sine function or about as expensive as the arcsine function, which both are parameterless, while KE has the parameter e .

Albeit we could eliminate all multiplications from the iteration loop, this is hardly honoured by current desktop computers, which nowadays have sophisticated multiplier units. Thus CORDIC algorithms have been displaced from computer processor. While our CORDIC KE solver is well competitive with Newton's method, its full potential would become available on architectures, which favour CORDIC methods, such as old or cheap devices. Also, a wider revival of CORDIC might be possible in the future.

ACKNOWLEDGEMENTS

I thank Hanno Rein for refereeing the paper, Trifon Trifonov for manuscript reading, and Albert Chan for helpful discussion about Barker's equation (Eq. (40), Sect. C). This work is supported by the Deutsche Forschungsgemeinschaft under DFG RE 1664/12-1 and Research Unit FOR2544 "Blue Planets around Red Stars", project no. RE 1664/14-1.

DATA AVAILABILITY

No new data were generated or analysed in support of this research.

REFERENCES

- Baykov V., 1972, PhD thesis, Leningrad State Univ. of Electrical Eng., <http://baykov.de/CORDIC1972.htm>
- Colwell P., 1993, Solving Kepler's equation over three centuries. Willmann-Bell, Richmond, VA
- Fukushima T., 1997, Celestial Mechanics and Dynamical Astronomy, **68**, 121
- IEEE 2008, IEEE Std 754-2008, pp 1–58
- Lang T., Antelo E., 2000, Journal of VLSI signal processing systems for signal, image and video technology, **25**, 19
- Meire R., 1985, Journal of the British Astronomical Association, **95**, 113
- Muller J., 2006, The CORDIC Algorithm. Birkhäuser Boston, Boston, MA, pp 133–156, doi:10.1007/0-8176-4408-3_7, https://doi.org/10.1007/0-8176-4408-3_7
- Payne M. H., Hanek R. N., 1983, SIGNUM Newsl., **18**, 18–21
- Takagi N., Asada T., Yajima S., 1991, IEEE Transactions on Computers, **40**, 989

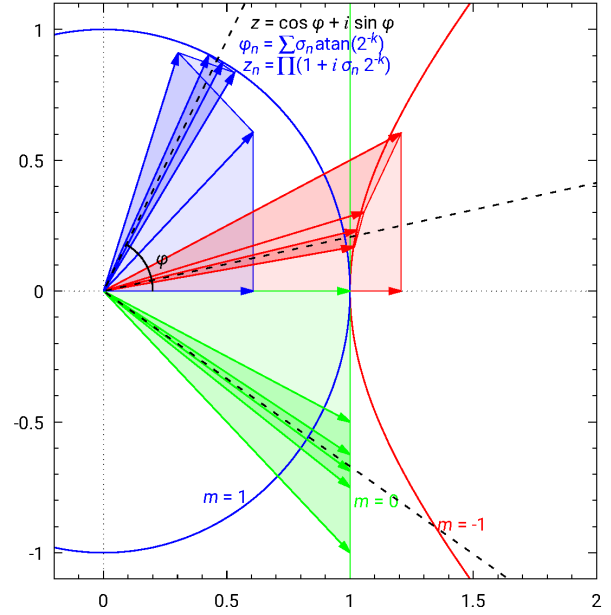


Figure A1. Examples of CORDIC rotations for circular (blue, $m=1$), linear (green, $m=0$), and hyperbolic mode (red, $m=-1$). The target angle φ (dashed line) is approached through rotations with $\alpha_n = \text{atan } 2^{-k}$. The vectors change their length with each iteration.

- Volder J. E., 1959, IRE Transactions on electronic computers, EC-8, 330
- Walther J. S., 1971, in Proceedings of the May 18-20, 1971, Spring Joint Computer Conference. AFIPS '71 (Spring). ACM, New York, NY, USA, pp 379–385, doi:10.1145/1478786.1478840, <http://doi.acm.org/10.1145/1478786.1478840>
- Zechmeister M., 2018, A&A, **619**, A128

APPENDIX A: NOTES ON THE CORDIC METHOD

Table A1 summarises the general output of CORDIC for the three coordinate systems m and the two operation modes. From this one can derive elementary functions using specific inputs as given in Table A2. For instance, the exp-function is obtained with $x_0 = K_h$ and $y_0 = K_h$ in hyperbolic vectoring (which is even simpler than adding the output of $x_0 = K_h$ and $y_0 = 0$: $\exp x = \cosh x + \sinh x$).

The logarithm is obtained from the atanh-function via the identity⁶

$$\ln \frac{a}{b} = 2 \operatorname{atanh} \frac{a-b}{a+b}.$$

So to compute $\ln a$, one has to set $b=1$, thus $x_0 = a+1$ and $y_0 = a-1$. The final multiplication with two is again a bitshift. The same mode provides simultaneously the square root \sqrt{a} . With $x_0 = a + \frac{K_h^2}{4}$ and $y_0 = a - \frac{K_h^2}{4}$, the output is directly available in x_n .⁷ The square root is independent of t , so this channel can be omitted.

For completeness, we list further important functions that can

⁶ $\tanh \ln \frac{a}{b} = \frac{\exp \ln \frac{a}{b} - \exp \ln \frac{1}{a/b}}{\exp \ln \frac{a}{b} + \exp \ln \frac{1}{a/b}} = \frac{\frac{a}{b} - \frac{1}{a/b}}{\frac{a}{b} + \frac{1}{a/b}} = \frac{a-b}{a+b}$

⁷ $\frac{K_h^2}{4} = 0.364512$. Usually, $x_0 = a + \frac{1}{4}$ and $y_0 = a - \frac{1}{4}$ are proposed to get \sqrt{a} . But this requires a post-multiplication with $\frac{1}{K_h}$.

Table A1. General input and output triples for various CORDIC modes (Walther 1971).

type	m	α_n	$\sum \alpha_n$	k_n	$K_{m,\infty}$	rotating ($t \rightarrow 0$)	vectoring ($y \rightarrow 0$)
linear	0	2^{-k_n}	2	$0 \dots N$	1	$\begin{bmatrix} x \\ y \\ t \end{bmatrix} \Rightarrow \begin{bmatrix} x \\ y+xt \\ 0 \end{bmatrix}$	$\begin{bmatrix} x \\ y \\ t \end{bmatrix} \Rightarrow \begin{bmatrix} x \\ 0 \\ t+y/x \end{bmatrix}$
circular	1	$\text{atan } 2^{-k_n}$	1.743 286	$0 \dots N$	0.607 253	$\begin{bmatrix} K_c x \\ K_c y \\ t \end{bmatrix} \Rightarrow \begin{bmatrix} x \cos t - y \sin t \\ x \sin t + y \cos t \\ 0 \end{bmatrix}$	$\begin{bmatrix} K_c x \\ K_c y \\ t \end{bmatrix} \Rightarrow \begin{bmatrix} \sqrt{x^2+y^2} \\ 0 \\ t + \text{atan}(y, x) \end{bmatrix}$
hyperbolic	-1	$\text{atanh } 2^{-k_n}$	1.118 173	$1 \dots N^*$	1.207 497	$\begin{bmatrix} K_h x \\ K_h y \\ t \end{bmatrix} \Rightarrow \begin{bmatrix} x \cosh t + y \sinh t \\ x \sinh t + y \cosh t \\ 0 \end{bmatrix}$	$\begin{bmatrix} K_h x \\ K_h y \\ t \end{bmatrix} \Rightarrow \begin{bmatrix} \sqrt{x^2-y^2} \\ 0 \\ t + \text{atanh}(y, x) \end{bmatrix}$

Notes. (*) Specific shift values k_n must be repeated, see Eq. (13).

Table A2. Input and output triples for some elementary CORDIC function m (-1 circular, 0 linear, 1 hyperbolic).

m	x_0	y_0	t_0	\Rightarrow	x_N	y_N	t_N
1	K_c	0	φ	$t \rightarrow 0$	$\cos \varphi$	$\sin \varphi$	0
-1	K_h	0	φ	$t \rightarrow 0$	$\cosh \varphi$	$\sinh \varphi$	0
-1	K_h	K_h	φ	$t \rightarrow 0$	$\exp \varphi$	$\exp \varphi$	0
1	1	b	0	$y \rightarrow 0$	$\frac{1}{K_h} \sqrt{1+b^2}$	0	$\text{atan } b$
-1	1	b	0	$y \rightarrow 0$	$\frac{1}{K_h} \sqrt{1-b^2}$	0	$\text{atanh } b$
-1	$a+b$	$a-b$	0	$y \rightarrow 0$	$\frac{2}{K_h} \sqrt{ab}$	0	$\frac{1}{2} \ln \frac{a}{b}$
-1	$a+1$	$a-1$	0	$y \rightarrow 0$	$\frac{2}{K_h} \sqrt{a}$	0	$\frac{1}{2} \ln a$
-1	$a + \frac{K_c^2}{4}$	$a - \frac{K_c^2}{4}$	0	$y \rightarrow 0$	\sqrt{a}	0	$\frac{1}{2} \ln \frac{4a}{K_h^2}$
0	a	0	φ	$t \rightarrow 0$	a	$\varphi \cdot a$	0
0	a	b	0	$y \rightarrow 0$	a	0	b/a

be derived with additional subsequent CORDIC calls

$$\tan x = \frac{\sin x}{\cos x} \quad \tanh x = \frac{\sinh x}{\cosh x} \quad (\text{A1})$$

$$\cot x = \frac{\cos x}{\sin x} \quad \coth x = \frac{\cosh x}{\sinh x} \quad (\text{A2})$$

$$\text{asin } x = \text{atan}(x, \sqrt{1-x^2}) \quad \text{asinh } x = \text{atanh}(x, \sqrt{x^2-1}) \quad (\text{A3})$$

$$\text{acos } x = \text{atan}(\sqrt{1-x^2}, x) \quad \text{acosh } x = \text{atanh}(x, \sqrt{x^2+1}). \quad (\text{A4})$$

For instance, $\tan x$ requires one division as a second call, whereas $\sin x$ and $\cos x$ come simultaneously from circular rotation. The arcsine is discussed in the next section.

A1 The arcsine function

From Eq. (A3) and Table A1, it can be seen that $\text{asin } x$ can be computed with hyperbolic vectoring, which provides the cathetus $\sqrt{1-x^2}$, and circular vectoring, which executes the atan function using two arguments and saves the division. Note, the cathetus needs a multiplicative scale correction (but see Sect. A2), implying three CORDIC calls in total.

A direct way to compute the arcsine is to change the direction decision as in Eq. (33) and to drive the y_n component of the vector towards the input argument. However, as explained in Muller (2006), the missing scale correction can lead to wrong decision and erroneous output as illustrated in Fig. A2. Baykov (1972) solved

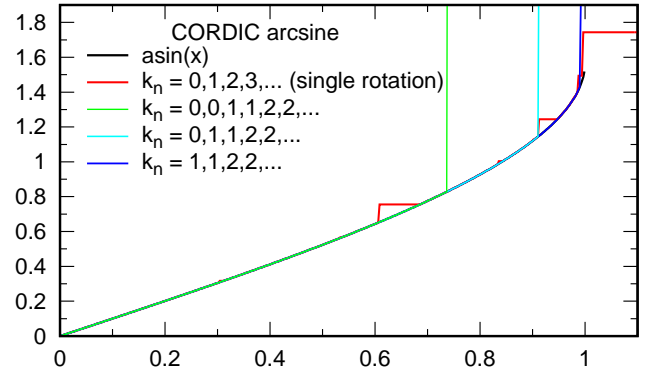


Figure A2. Output of the arcsine mode. Single rotations (red) have overall convergence problems. The three double rotation sequences (green, cyan, blue) converge in a limited range. Full convergence is achieved by three chained CORDIC operations or double iterations with quadrant check or scale correction (black, barely visible in right corner).

the problem with double iterations, meaning each iterations is executed twice. However, just using the sequence $k_n = 0, 0, 1, 1, \dots$ converges only for $|x| < 0.73$, because after the third rotation the vector cannot recover from an excursion into an adjacent quadrant. The sequences $k_n = 0, 1, 1, 2, 2, \dots$ or $k_n = 1, 1, 2, 2, \dots$ have a larger convergence range (related to a smaller total scale corrections). But only an additional quadrant check ($x_n > 0$) in each iteration gives full convergence including the arcsine-corner. We remark that Kepler's equation is bijective and thus does not suffer from quadrant confusion.

Takagi et al. (1991) developed an alternative method, which is also called double-CORDIC iteration and employs an auxiliary variable, which is scale corrected on the fly. Lang & Antelo (2000) also uses an on the fly correction, but do not require double rotations.

In summary, there are different ways to compute the arcsine. They may require modifications and the total costs correspond to about 2–3 normal CORDIC cycles.

A2 Multiplication and division with a constant

The standard CORDIC algorithm requires a scale correction. The scale correction does not matter in the output t_N , where the factor cancels out in the ratio y/x in all modes. But a pre- or post-scaling

Code B.1: Fix-point algorithm with CORDIC double iteration for Kepler's equation.

```

1 from math import atan, tau
2
3 kmax = 53      # largest shift value
4 R = 1 << 61    # binary point
5
6 ak = []        # atan lookup table
7 K = 1          # scale correction factor
8 for k in range(kmax+1):
9     ak += [(atan(2**k), k)]
10    if 2*k <= kmax:
11        K /= 1 + 4**k
12        ak += ak[-1:]
13
14 KR = K * R
15 i64_ak = [(round(a*R), k) for a,k in ak]
16
17 def i64_Ecs(M, e):
18     t = M - tau*round(M/tau)
19     t = round(t * R)
20     x, y = round(KR*e), 0
21     for a,k in i64_ak:
22         s = t+y >> 63
23         t -= s ^ s + a
24         x, y = x - (s^s+(y>>k)), \
25             y + (s^s+(x>>k))
26     return M+y/R, x/R, y/R

```

is needed, when using the output x_N or y_N in the modes $m=1$ or -1 .

CORDIC provides multiplication and division, and their execution requires a full CORDIC cycle. However, if the multiplier is known in advance and often needed, the efforts can be reduced.

Let's consider first a division by 3, which occurs in Eq. (40). The binary representation of $\frac{1}{3}$ is 0.01010101₂..., thus its multiplication can be done as $(2^{-2} + 2^{-4} + 2^{-6} + 2^{-8} + \dots)$. The corresponding shift-and-add algorithm (essentially a binary multiplier) can be seen as a CORDIC simplification, which needs only half iterations, because the iterations with odd shift values can be omitted, since the linear mode is scale free. Moreover, it does not need direction decisions and the t channel, because the multiplier is encoded in the shift sequence. The bit shifts can be done in parallel.

Multiplications with other important constants, in particular the scale correction $K_c \approx 0.100\,110\,110\,111\,010_2$ and $K_h \approx 1.001\,101\,010\,001\,111_2$, could be implemented in a similar way.

APPENDIX B: CODE ILLUSTRATION

In the following, we document a fix-point implementation of the CORDIC double iteration. The pure Python code shall illustrate the functionality and low complexity. Further variants (floating-point) and other programming languages, in particular more performant, low-level C, are maintained online*.

Code B.1 implements the algorithm described in Sect. 3. In this snippet, the largest shift is hardcoded in line L 3 and thus sets the number of iterations. The precision depends furthermore on the

Code B.2: Fix-point algorithm with CORDIC double iteration for hyperbolic Kepler's equation.

```

1 from math import atanh, frexp, log
2 ln2 = log(2)
3
4 kmax = 53      # largest shift value
5 R = 1 << 61    # binary point
6
7 ahk = []       # atanh lookup table
8 Kh = 1         # scale correction factor
9 for k in range(1, kmax+1):
10    ahk += [(atanh(2**k), k)]
11    if 2*k <= kmax:
12        Kh /= 1 - 4**k
13        ahk += ahk[-1:]
14
15 KhR = Kh * R
16 i64_ahk = [(round(a*R), k) for a,k in ahk]
17
18 def i64_Hcs(M, e):
19     m = max(0, frexp(M/e)[1])
20     eK = round(e * KhR) >> 1
21     x = (eK<<m) + (eK>>m)
22     y = (eK<<m) - (eK>>m)
23     if M < 0: m, y = -m, -y
24     t = M + m*ln2
25     t = -round(t * R)
26     for a,k in i64_ahk:
27         s = -t-y >> 63
28         t -= s ^ s + a
29         x, y = x + (s^s+(y>>k)), \
30             y + (s^s+(x>>k))
31     return y/R-M, x/R, y/R

```

location of the binary point (Sect. 5.1)⁸ defined in line L 4. The lookup table (L 6, L 9) stores the tuples of the basis angles and the shift sequence ($\alpha_n = \text{atanh}(\frac{1}{2^{k_n}}, k_n)$). If the correction term 4^k in Eq. (9) is numerical yet larger than 2^{k_N} (L 10), i.e. $k \leq k_N/2$, the required scale correction is accumulated (L 11) and the last table entry is repeated (L 12). Then the table and the scale factor are converted to fix-point (64 bit integers, L 14–L 15). The input of algorithm are floating-point numbers. Thus after a simple range reduction in L 18 (note that there are more accurate range reduction algorithms, Payne & Hanek 1983) and pre-scaling with K , the start vector is converted to fix-point (L 19–L 20). The multiplication $e * K$ (L 20) is the only true multiplication (but see Sect. A2). (The multiplication with R and integer conversion can be done with mantissa extraction and bit shift).

The CORDIC iterations start in L 21. The comparison of Eq. (17) is done by an addition and a subsequent arithmetic right bit shift, which extracts the sign bit (L 22). The variable s is either 0 or -1. The bitwise operation $s \wedge (s+x)$ (alternatively $(x \wedge s) - s$) modifies the sign of x in a branchless fashion. In case of $s=0$ ($\sigma_n = 1$), the variable x is not modified. In case of $s=-1$ ($\sigma_n = -1$), the result is an arithmetic negation ($-x$, see also Table 1). This can be directly implemented in hardware (adder-subtractor). Line L 23 accumulates

⁸ Because Python integers have arbitrary precision, calculations beyond 64 bits would be possible by increasing this number.

the angles as described in [Sect. 5.4](#). Finally, the fix-point numbers are converted back to floating-point ([L 26](#)).

As an example, calling the function with `i64_Ecs(2-sin(2), 1)` should return the triple `(2.0, -0.41614683654714246, 0.9092974268256817)`.

The code for the hyperbolic Kepler equation ([Sect. 4](#), [Code B.2](#)) is very similar. It requires the hyperbolic arctangent ([L 10](#)). The range extension is done in [L 19–L 22](#).

APPENDIX C: BARKER’S EQUATION

The equivalence of Eqn. [39](#) and [40](#) follows from

$$B - \frac{1}{B} = e^{\ln B} - e^{-\ln B} = 2 \sinh \ln B \quad (\text{C1})$$

$$= 2 \sinh \ln \sqrt[3]{W + \sqrt{W^2 + 1}} = 2 \sinh \frac{\operatorname{asinh} W}{3}. \quad (\text{C2})$$

The last step employed the identity (e.g. [Fukushima 1997](#), Eq. (73))

$$\operatorname{asinh} x = \ln \left(x + \sqrt{x^2 + 1} \right), \quad (\text{C3})$$

which itself can be verified with the substitution $x = \sinh t$

$$t = \ln \left(\sinh t + \sqrt{\sinh^2 t + 1} \right) = \ln \left(\sinh t + \sqrt{\cosh^2 t} \right) \quad (\text{C4})$$

$$= \ln (\sinh t + \cosh t) = \ln e^t = t. \quad (\text{C5})$$